INTERNATIONAL JOURNAL OF AUTOMOTIVE AND MECHANICAL ENGINEERING (IJAME)
ISSN: 2229-8649 e-ISSN: 2180-1606
VOL. 19, ISSUE 2, 9747 – 9758
DOI: https://doi.org/10.15282/ijame.19.2.2022.10.0752

ORIGINAL ARTICLE

Experimental and Numerical Studies on the Development of Hysteresis in a Shock Absorber with a Shim Disc Valve

D. Buczkowski[1,*], S. Zymelka[2] and G. Nowak[1]

[1]Department of Power Engineering and Turbomachinery, Silesian University of Technology, 44-100 Gliwice, Poland
[2]Department of Machine Technology, Silesian University of Technology, 44-100 Gliwice, Poland
Phone: +48663933769

ABSTRACT – The paper describes the observed occurrence of hysteresis of the characteristic curve of a shock absorber valve. The phenomenon has an impact on the asymmetry of the damping force characteristic and should be taken into account when modelling the valve operation. The aim of the investigations was to determine the factors generating the phenomenon and establish the relationships between these factors and the hysteresis size. Tests were carried out on a stand intended for valve measurements in isolated conditions. A strongly coupled Fluid-Structure Interaction numerical model was also created to simulate the valve operation in selected conditions. The results indicate that the hysteresis loop occurrence is mainly due to the conditions of the valve disc stack preload in the process of its composition and, consequently, to the friction between the valve elements. Having an impact on the contact between discs and on the disc stack overall structure, they affect the hysteresis field significantly. The testing results confirm the supposition that hysteresis is not due to the phenomena related to the conditions of the flow through the valve.

ARTICLE HISTORY
Received: 2nd Apr 2021
Revised: 12th Apr 2022
Accepted: 10th June 2022
Published: 28th June 2022

KEYWORDS
Fluid-structure interaction;
CFD;
Numerical model;
Shock absorber;
Hysteresis

INTRODUCTION

The car suspension system has attracted the interest of researchers for a long time because its influence on vehicle stability, handling characteristics, and passenger comfort is of key importance. Due to its multidimensional functions, it is considered to be one of the most important systems in the vehicle structure. The car suspension consists of a system of springs, shock absorbers and links that integrate the vehicle with the wheels. The primary function of the vehicle suspension is to support the vehicle body and ensure drive and ride comfort [1]. The key element of the suspension system is the shock absorber, which, among other things, has an impact on the vehicle position, traction and response to the steering system. In addition, it has to provide comfort to the passengers by reducing vibrations and noise. Typically, achieving these qualities requires a compromise between the comfort of passengers and vehicle behaviour, both of which have to be taken into account while developing the shock absorber damping characteristics.

In order to meet those contradictory requirements, the designers of shock absorbers have to introduce non-linearity into their performance characteristics. What is more, an asymmetrical level of damping forces can usually be observed between the shock absorber compression and rebound strokes, as can be observed in Figure 1. The car behaviour on the road is, to a large extent, dependent not only on the absolute values of forces that can be read from the diagrams but also on the shape of the curves illustrating their history. The shape is affected by a number of phenomena and dynamically changing operating conditions. A characteristic disturbance of the theoretical damping force curve is the occurrence of hysteresis loops. Among other things, they are due to the compressibility of the damping medium, elastic susceptibility of the walls of the shock absorber chambers and the oil aeration and cavitation phenomena.

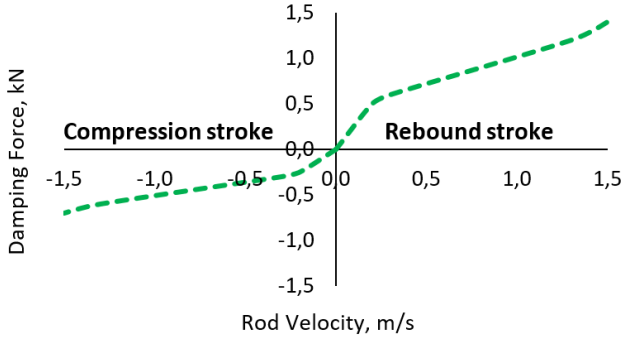

Figure 1. Example non-linear curve of the damping force-velocity characteristic.

*CORRESPONDING AUTHOR | Buczkowski D. | ✉ dbuczkowski@driv.com

Moreover, the actual level of forces generated by the shock absorber can vary depending on the dynamics of the induction of the motion, i.e. the induction frequency and amplitude. Considering their individual complexity, the above-mentioned factors affecting the shock absorber performance are usually investigated independently. In [3], the authors point to the conditions in which the oil aeration phenomenon occurs and the impact it has on the shock absorber performance. They draw attention to two effects that testify to the occurrence of aeration: the characteristic delay in the build-up of damping forces in the initial phase of the stroke and the hysteresis loop caused by a sudden change in the fluid compressibility.

In [4], Pavlov described and investigated the effect of variable temperature conditions on the level of forces generated by the shock absorber, as well as the absorber responsiveness and the frequency response. The impact of temperature is noticed in the entire range of the rod stroke, and it is found to be independent of the nature of the flow induction. The temperature conditions in the shock absorber chambers can change dynamically due to strong variations in loads and heat removal conditions [5]. The damping force is usually calculated using the fluid dynamics theory under the assumption that the applied oil is incompressible. Lang [6] considered the oil compressibility in a mathematical model of the shock absorber. Both simulations and experiments indicate that oil compressibility is one of the main causes of the shock absorber's non-linear dynamic behaviour, such as hysteresis loops occurring at higher values of induction frequency. Another aspect of the research is the inertia of oil and the valve elements [7].

Most of the works on the damping curve hysteresis phenomenon are carried out at the system (damper) level. They are based on experimental data which try to simulate the shape of the characteristics using one-dimensional mathematical/system models and appropriate sets of parameters [8], [9], [10]. Such an approach has many advantages, e.g. analysis of the interaction between components, a multiplicity of levels of the models (valve-shock absorber, suspension-vehicle) or a combination of many fields of physics. On the other hand, it involves certain limitations which can be seen at the level of individual components. To simulate them accurately, it is necessary to provide input data obtained from experiments; such models are correlated at the target level, e.g. of the shock absorber, which may produce ostensible correlation achieved by using incorrect values of input parameters. The models then run the risk of losing credibility if the analysed case differs from the model that was correlated with the test data (e.g. a different valve). Therefore, system-level modelling is mainly used to analyse different types of induction forces acting on the model, while it does not determine the effect of design changes on the system.

This work is focused on the phenomenon of the occurrence of the damping curve hysteresis loop. The testing was carried out on an experimental stand, and then a prepared coupled numerical model was used. The aim of this work is to identify the main cause of the hysteresis loop occurrence in the case under analysis and determine the factors having an influence on the hysteresis loop presence and intensity. The testing was carried out based on a real shock absorber design characterised by the occurrence of the described phenomenon. Modelling the operation of a valve showing hysteresis loops by means of the FSI numerical analysis is a novel approach to the problem. The valve studies using strongly coupled FSI numerical analyses have so far focused on the determination of the basic flow characteristics for various flow inductions [11], [12]. This paper describes a new alternative way of taking account of the valve disc stack preload in numerical simulations, which can be realised at the existing limitations of the process of coupling solvers in the ANSYS System Coupling. By comparing the results of the numerical analysis with the experimental data, it was possible to accurately simulate the phenomenon in the computer model used for the presented analyses.

SHOCK ABSORBER VALVE UNDER CONSIDERATION

The study concerns a compression valve connecting the inner chamber to the reserve chamber of a twin-tube shock absorber whose design and principle of operation are described in [13], [14]. It is a non-return valve, which means that the flow during the rebound stroke is controlled only by a check valve, which allows a free flow in one direction. During the compression stroke, oil flows through channels closed by a set of discs, supported by a washer and clamped in the process of crimping the end of the valve pin. The damping forces are adjusted by selecting the disc stack composition, i.e. the number, diameter and thickness of the discs. An example view of the valve under consideration is presented in Figure 2.

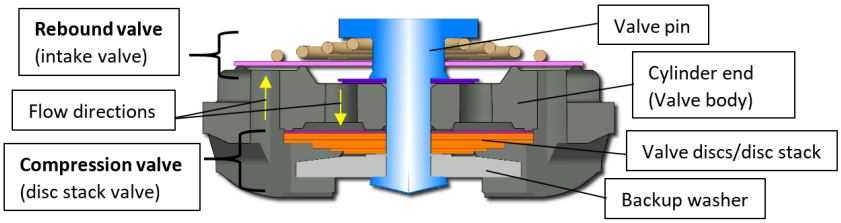

Figure 2. View of the compression valve cross-section.

This valve design was identified as the cause of the hysteresis loop occurrence in the characteristic curve of the analysed shock absorber. The valve design used in the shock absorber, whose characteristic curve showed considerable hysteresis loops, was measured on a stand intended for the measurement of the damping curve in isolated conditions. The stand is described in the next section. On the flow rate-pressure diagrams presented in Figure 3, it can be seen that the hysteresis loop occurs only for the oil flow in the direction of the compression stroke. It is therefore concluded that the

check valve design has no impact on the hysteresis occurrence and the only reason for it is the operation of the compression valve in the form of a stack of clamped discs. These results made the authors conduct a detailed analysis of the presented problem using FSI modelling. The focus of the efforts is on simulating the operation of the valve individual components, the interaction between them and the impact of their geometry on the generated damping forces.

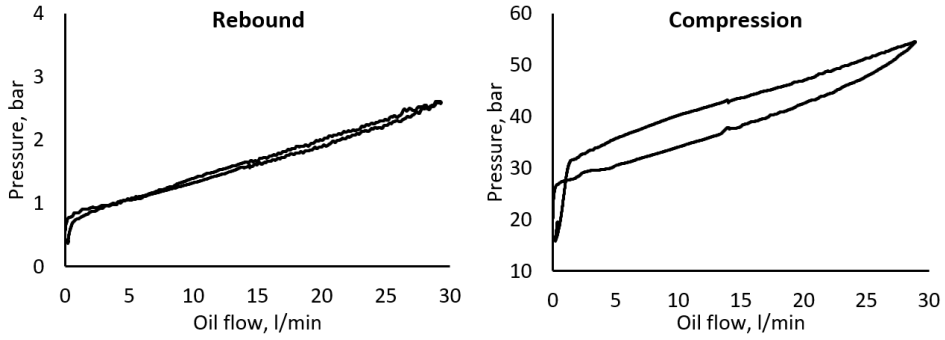

(a) (b)

Figure 3. Compression valve flow characteristics at the (a) rebound and (b) the compression stroke direction.

MEASUREMENTS ON THE TEST BENCH

The testing of the impact of different configurations of the discs on the occurrence of the hysteresis loop phenomenon was carried out on a test bench enabling isolation of the valve operating conditions. The stand design makes it possible to isolate the tested valve from the impact of the shock absorber other features, such as the characteristic of another valve or elastic susceptibility of the walls of the valve chambers. It is built of a metal column in which the tested valve is placed. In the case of the compression valve of a twin-tube shock absorber, at the preparation stage, it is fixed on the end of a tube corresponding to the shock absorber inner tube and mounted in the column on a purpose-made bottom with holes. Two oil-flow channels are connected to the column. The flow is ensured by two pumps working in parallel, a low- and a high-flow pump. Standard oil, typically used to fill shock absorbers, is used in the bench hydraulic system. The pressure drop on the tested valve was measured at the column outlet on the oil inflow and outflow channel.

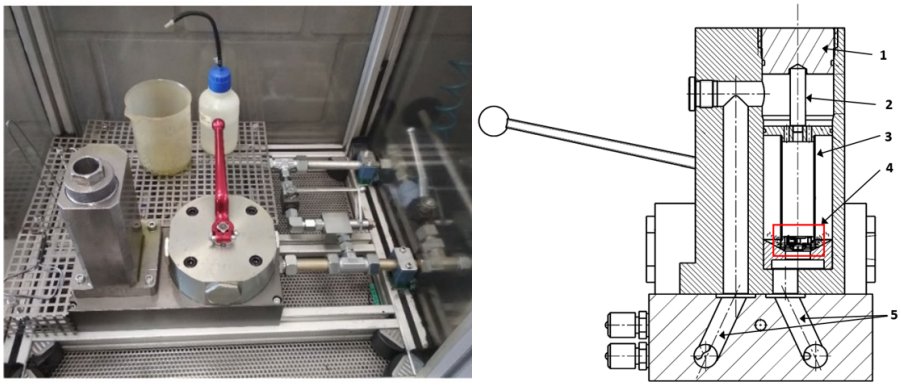

(a) (b)

Figure 4. (a) flow test bench, (b) cross-section of the metal column: 1 – sealed nut, 2 – pin, 3 –inner tube, 4 – valve location, 5 – inflow/outflow channel.

Knowing that the analysed valve generates significant hysteresis loops, a decision was made to investigate the effect of other disc combinations. For this purpose, the flow characteristics of four compression valves with different disc stack compositions were measured. The selected disc sets are presented in Table 1. Valve 1 was chosen as the reference valve with a disc stack combination corresponding to the valve where the phenomenon was observed. All the discs used to make the valves were full with no cuts generating bleeds (cf. bleed discs or orifice discs).

Four valve designs were composed according to the data from Table 1. On the rebound valve side, a check valve was installed to close the flow channels for the rebound stroke, which can be seen in Figure 2. On the compression valve side, the disc stack was closed with a washer and clamped in the valve pin crimping process, which ensured the clamping force at the level of ~5 kN. Prior to the test, the bench hydraulic system was vented. The flow rate was set as varying linearly in the range of 0-30 l/min. The pressure generated by the valves was measured during the flow rate increase and decrease. The oil flow was realised in the direction of the compression stroke of the rod. The oil used in the measurements was taken from a tank with a constant temperature of 25 ºC. Each valve version was measured three times. Due to the low dynamics of the flow induction (flow rate increase and decrease in >2.0 sec.), it can be assumed that the test conditions were quasi-static. The measurement results were obtained in the form of curves illustrating the pressure drop on the valve

as a function of the volumetric flow rate. The results for the tested disc stack compositions are shown on the graph in Figure 5 (the scale of the Y-axis was truncated for better clarity of the results).

Table 1. Disc stack compositions considered for the measurement.

Component name	Valve 1	Valve 2	Valve 3	Valve 4
Cylinder End	common component			
Disc 1	17.6x0.15	17.6x0.15	17.6x0.15	17.6x0.15
Disc 2	17.6x0.15	17.6x0.20	17.6x0.15	17.6x0.15
Disc 3	17.6x0.15	17.6x0.25	15.3x0.20	17.6x0.15
Disc 4	17.6x0.15	17.6x0.25	15.3x0.20	17.6x0.15
Disc 5	17.6x0.15	-	14.4x0.20	17.6x0.15
Disc 6	17.6x0.20	-	13.0x0.15	17.6x0.15
Disc 7	17.6x0.25	-	12.0x0.20	17.6x0.15
Disc 8	-	-	-	17.6x0.15
Backup Washer	common component			

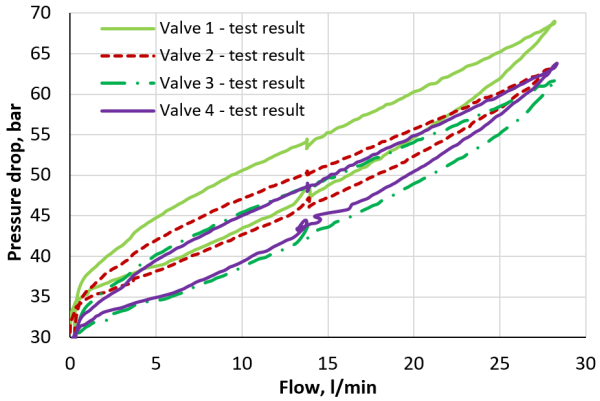

Figure 5. Results of experimental measurements.

The presence of hysteresis fields during the measurements on the described test stand allowed a preliminary rejection of several potential hypotheses concerning the origin of the phenomenon. Considering the structure of the stand and the method of measurement, aeration could not have been the cause of the hysteresis loop of the characteristic curve. The presence of aeration translates into a delay in the valve opening and an occurrence of a hysteresis loop in the initial range of the characteristic curve [3], which is not observed in the performed experiment. There is no dynamic change in the direction of the oil flow during the measurement, and the pressure in the pumped oil chamber never drops to the limit of the oil saturation with gas. It is therefore concluded that the measurement method excludes the possibility of the occurrence of aeration conditions. The stand design also excludes the influence of elastic compliance of the walls of the shock absorber chambers. The column in which the valve is mounted is not susceptible to deformation in the pressure ranges under consideration. Oil compressibility was also rejected as the cause of hysteresis formation. The dynamics of the flow excitation during the measurement are too low (<1 Hz), and the oil compressibility impact is visible for high-frequency load excitations [6]. Moreover, the hysteresis loop occurring in the whole linear range of the characteristic curve (the valve disc performance curve) does not correspond either in shape or location to the hysteresis field, which is caused by fluid compressibility and which can be observed in [6], [7],[8].

At a flow rate close to 15 l/min, a continuity disturbance can be observed on the experimental curves. It is caused by the high-flow pump activation/deactivation and should not be associated with the operation of the valve itself. Comparing the characteristic curves of the tested valves, it can be noticed that the widest field of hysteresis occurs for the stiffest valve, with all discs having the same diameter (Valve 1). All the valves under analysis are characterised by a similar level of preload determining the opening pressure, which is included in the range of 32-37 bar. The narrowest hysteresis field occurs for Valve 2, which has the smallest number of discs. The obtained results suggest that the hysteresis field depends to some extent on the composition of the discs or the design of the valve itself. The reasons, however, should not be sought in the flow conditions or the damping fluid parameters.

NUMERICAL MODEL

In order to better understand the causes of the hysteresis loop occurrence in the considered valve type, it was decided to create a numerical model of the compression valve. In principle, the operation of a valve of this type involves continuous interaction between the flowing oil pressure and the deformation state of the set of discs. The slope of the damping force curve, as well as the pressure initiating the valve opening, depending on the stiffness of the disc set and the preload due to the clamping force. Due to the strong dependence of the flow conditions on the deformation of elastic components of the valve, it was decided to use a coupled approach – the fluid-structure interaction (FSI) method. The FSI is a multi-physical issue involving interaction between the domains of the solid and of the fluid. This is understood as

structural deformation under the impact of pressure forces occurring in the fluid domain. As a result, the fluid field is changed to adapt to the new shape of the structure.

In numerical analyses, coupling is realised in a separable approach, which makes it possible to apply an appropriate solver independently for each field of physics being simulated, using the model discretisation and the numerical algorithm suitable for the fields. The interaction between them is realised by an external coupling algorithm [15]. Two integration strategies are available for the coupled problem: an explicit method (loose coupling over time) and an implicit or strongly coupled method. The choice of the method will depend on the specificity of the problem to be solved. The explicit procedure involves solving the flow field and the structure field once sequentially and moving to the next time step without imposing convergence conditions at the end of each step. Due to its simple and modular implementation, this method is widely used in aeroelasticity calculations, where the coupled dynamics is often determined by the vibration characteristics of the structure [15], [16], [17].

Implicit schemes, on the other hand, require that the two modules solving individual fields satisfy convergence conditions imposed on the exchanged data, both between each other and at the end of each time step. In order to achieve this during each time step, the data exchange between the solvers is carried out iteratively, and during each iteration, the program performs calculations based on updated boundary conditions [18]. Owing to that, the model based on this scheme makes it possible for each solver to take account of the dynamics of the simulated phenomenon. The difficulties arising from this approach usually concern the capturing of considerable deformations with high dynamics, which requires a sufficiently small time step to ensure convergence of the solution. As a result, this can lead to a significant lengthening of the time needed to complete the analysis or increase the demand for computational power.

The use of an explicit/weak coupling scheme or unidirectional coupling is described in the context of valve research in works such as [14], [19]. The authors obtained results of the flow characteristics of the tested valve but under the assumption that the flow path adopted in the CFD model corresponds to the estimated shape of the structure under load. Such solutions are only acceptable in cases where the structure deformations or loads can be determined in advance in a reliable way. Otherwise, this approach may result in a non-physical solution.

In the case under consideration, due to the need to capture the dependence of the flow parameters on the stiffness of the disc stack over the entire range of the analysed flow rates, an implicit solution scheme was applied. The strong coupling-based approach is described in [20]. The authors created a numerical model that made it possible to capture dynamic characteristics of the flow through the valve taking account of the current strain-and-stress state of the discs. In [11], the authors proved that a strongly coupled FSI model could successfully be applied to simulate the damping curve. They obtained a good correlation of the simulation results with the experimental data, and the proposed model can be used successfully to optimise the analysed structure. The above-mentioned works made the authors of this paper build a strongly coupled numerical FSI model to simulate the operation of the tested valve.

Fluid Dynamics (CFD) Model

The issue under consideration is the incompressible fluid turbulent flow, described by the Reynolds-averaged Navier-Stokes (RANS) equations and by continuity equations, Eq. (1), Eq. (2). They describe, in a differential form, the principles of mass and momentum conservation in the fluid:

$$\rho \partial v_i/\partial t + \rho v_j \partial v_i/\partial x_i = -\partial p/\partial x_i + \mu \partial^2 v_i/\partial x_j \partial x_i + \rho b_i \tag{1}$$

$$\partial \rho/\partial t + \rho \, \nabla \cdot v = 0 \qquad \text{and} \qquad \partial \rho/\partial t = 0 \tag{2}$$

where v_i and v_j are the fluid averaged velocities, p is pressure, μ is dynamic viscosity, and b_i is responsible for external forces. The equations are complemented with an appropriate turbulence model to capture the presence of the flow large- and small-scale swirling. The choice of the appropriate turbulence model depends on the flow field occurring in a given case.

In industrial applications, the most commonly used are the URANS (Unsteady-RANS), two-equation models from the group of k-ε or k-ω models [21], [22]. They enable significant savings in computational power compared to detailed Direct Numerical Simulation (DNS) or partially simplified Large Eddy Simulation (LES) methods of turbulence modelling [23], [24]. For the purpose of this numerical model, it was decided to use the Realisable k-ε model, which is an improved version of the Standard k-ε model. It was well described by the authors of [25], who adapted it to analyse the influence of the channel topology on the level and nature of the flow turbulence. The Standard k-ε model is a semi-empirical model based on transport equations for turbulent kinetic energy (k) and its dissipation rate (ε). Although widely used, it has certain drawbacks. The Realisable k-ε model differs from the Standard model in two essential aspects. Firstly, the Realisable k-ε model includes a new formulation of the turbulent viscosity equation. Additionally, a new transport equation for the k-ε dissipation rate was derived from the exact equation for the transport of the mean-square vorticity fluctuation.

$$\frac{\partial}{\partial t}(\rho k) + \frac{\partial}{\partial x_j}(\rho k u_j) = \frac{\partial}{\partial x_j}\left[\left(\mu + \frac{u_t}{\sigma_k}\right)\frac{\partial k}{\partial x_j}\right] + G_k + G_b - \rho\varepsilon - Y_m + S_k \tag{3}$$

$$\frac{\partial}{\partial t}(\rho\varepsilon)+\frac{\partial}{\partial x_j}(\rho\varepsilon u_j)=\frac{\partial}{\partial x_j}\left[\left(\mu+\frac{u_t}{\sigma_\varepsilon}\right)\frac{\partial\varepsilon}{\partial x_j}\right]+\rho C_1 S\varepsilon-\rho C_2\frac{\varepsilon^2}{k+\sqrt{v\varepsilon}}+C_{1\varepsilon}\frac{\varepsilon}{k}C_{3\varepsilon}G_b+S_\varepsilon \quad (4)$$

In Eq. (3) and Eq. (4) presented above, G_b denotes generation of kinetic energy turbulence due to buoyancy, G_k is the generation of kinetic energy turbulence due to mean velocity gradients, Y_m is the share of dilatation fluctuation in compressible turbulence at the general dissipation rate, and σ_k an σ_ε are turbulent Prandtl numbers. The values of constants specific to the Realizable k-ε model are as follows: $C_{1\varepsilon}$ = 1.44, $C_{2\varepsilon}$ = 1.92, σ_k = 1.0, σ_ε = 1.3, and C_μ = 0.09. In order to reduce the model sensitivity to the boundary layer mesh resolution, the Enhanced Wall Treatment (EWT) function was used. If the size of the mesh elements is adequate for calculations related to the behaviour of the boundary layer (y+ ≈ 1), a traditional two-layer model is used. In the case of a coarse mesh, the Enhanced Wall Treatment option is applied [21]. This method enables a reduction in the number of mesh elements in regions which are not essential from the perspective of the objective of the analysis.

The CFD model was prepared using the ANSYS Fluent 2020 software package. The fluid domain was discretised using a tetrahedral unstructured mesh with second-order elements. The boundary layer was modelled as eight rows of wedge-type elements on its thickness. In the region of the gap between the disc and the cylinder end, where the biggest velocity and pressure gradients are expected, a much denser numerical mesh is used. In order to check the solution independence of the numerical mesh, an analysis was conducted of the solution sensitivity to the mesh element size by performing calculations on meshes with 120,000 - 450,000 elements. Based on that, it was estimated that the model mesh with 210,000 elements (element size: 0.02 – 0.1 mm) could produce reliable results in the range of the analysed flow rates. In the area of contact between the first disc and the surface of its support on the cylinder end (the valve body), a thin oil film with a thickness of 20 µm was modelled. Such a gap pre-filled with oil makes it possible to solve the difficult aspect of closed contact between surfaces filled with oil after opening. A similar approach was successfully used by the authors of [19] for the same purpose. It was assumed that the size of the gap was too small to have a significant effect on the flow characteristics.

The next step was to define the mesh deformation method, which is crucial for the solution convergence. Smoothing was used, which is the basic method of adapting the mesh shape to problems with moving or deformable boundary walls. The surface nodes lying exactly on the boundary are moved to conform to the new position or shape of the surface. Their displacement affects the position of neighbouring internal nodes according to the adopted smoothing model and its parameters. This method was sufficient for the analysed cases due to the relatively small deformation of the discs during the opening and the adequate volume of the mesh in the neighbourhood. As a result, the deformations of the mesh edges were freely compensated for in consecutive layers of the elements without deteriorating the mesh quality.

The oil properties that were input into the model correspond to the oil used in the experiment according to the supplier's specifications: density – 860 kg/m^3, dynamic viscosity – 0.017Pa-s at the temperature of 25°C. The flow excitation was described in the form of a UDF file. The flow rate was linearly increased and decreased between 0 and ~30 l/min and only took place in the direction corresponding to the direction of the rod compression stroke – from the beginning of the stroke to its stop.

Transient Structural Model Setup

The shape of the valve elements allowed the use of axisymmetric modelling. However, due to the requirements of the software used to exchange data between solvers (2D not supported), the model had to be made as a 3D circular sector, with the angular width limited to 2º. The structural model (FEA) was built and analysed using the ANSYS Mechanical 2020 software package. The discrete model of the valve included hexahedral disc meshes, consisting of 4 elements on the disc thickness. The deformations of the cylinder end and of the washer are negligible; therefore, these components were treated as rigid bodies. The valve discs were modelled as elastic components, to which the following material properties were assigned: Young's Modulus: 210 GPa and Poisson's Ratio: 0.3. Plastic deformation of components is unacceptable within the range of the shock absorber operating conditions. No such deformation was observed during the performed experimental measurements, either. The contact between the components, as frictional, was solved using the augmented Lagrange method. The friction factor of the contact was analysed in the next steps.

The disc stack valve type is commonly characterised by an initial preload condition that is coming from a difference in height of support regions (between the outer and inner diameter of the disc stack) and the compression of the discs on their inner diameter due to the crimping of the pin or nut torqueing. Unfortunately, due to the need to define the boundary conditions within a single step (required consistency between CFD/FEA solvers), it is impossible to apply the dedicated *bolt pre-tension* option (ANSYS Mechanical) simulating the clamping of discs. This is because the *bolt pre-tension* option requires a minimum of 3 steps to fully define the following quantities: the initial displacement, the clamping force and the displacement lock. On the other hand, the boundary condition assuming completely rigid support of the disc stack results in overestimation of the support reactive force. Such a simplification was made in [26] and it was recognised as one of the main reasons behind the overestimation of the pressure results generated by their numerical model. Nevertheless, the structure they investigated was indeed substantially simplified: no interaction between the valve discs (one disc obscuring the flow), no disc preload. For the compression valve design analysed herein, accurate mapping of the valve preload conditions is of key significance for the correctness of the results.

In the structural model used in the following study, the disc stack clamping was simulated using an alternative method. The process was modelled using a spring element connected to the washer, according to Figure 6. In the first step of the simulation, the spring was compressed by a specific distance (based on the spring rate value). As a result, the generated

force was transferred through the washer to the whole structure until the desired level of the reactive force, between the disc stack and valve body was achieved. The reactive force represents the clamping force coming from the valve pin crimping during the process of the valve composition. Such an approach ensures that flow pressures acting on the discs stack are counteracted with appropriate reaction force from the support (washer), and at the same time, initial discs compression is included.

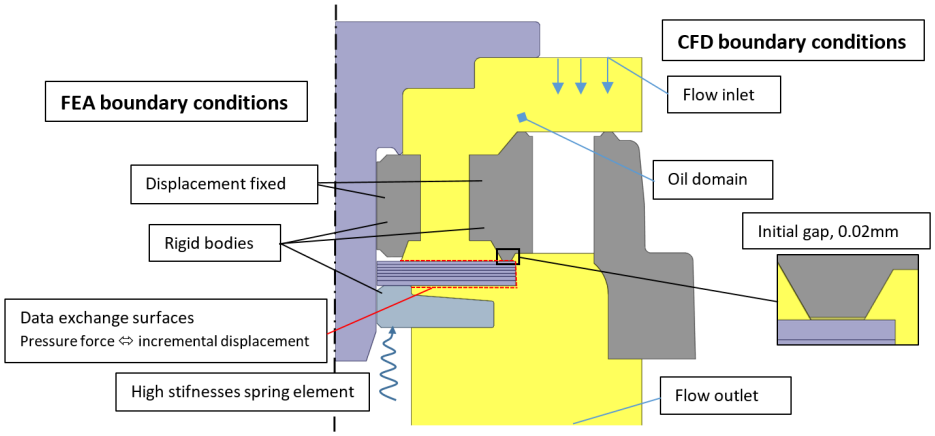

Figure 6. Example illustration of the numerical model boundary conditions.

Fluid-Structure Solver Coupling

In order to realise the data transfer during a strongly coupled bidirectional simulation (implicit scheme), the System-Coupling module is available in the ANSYS Workbench. Feature working principles are described in details in [27] was used. In this module, the flow solver (Ansys Fluent) and the structural solver (Ansys Mechanical) were combined. The fluid mechanics equations: the Reynolds-averaged Navier-Stokes (RANS) equations with the Realisable k-ε turbulence model are solved in the computational domain using the CFD solver. The obtained pressure forces are exported as loading conditions to the transient structural solver. Based on updated loads, the current stress-and-strain state of the structure is determined in the structural analysis. Depending on the criteria defined for the data exchange between the solvers (number of data exchange iterations/criterion for the exchange convergence), the CFD model mesh is updated based on the imported deformations of the structure, and the case is recalculated, or a transition is made to the next time step. The order of the data exchange can be changed depending on the needs of the task under analysis. The data exchange is realised based on the model topology (surface-to-surface in this case).

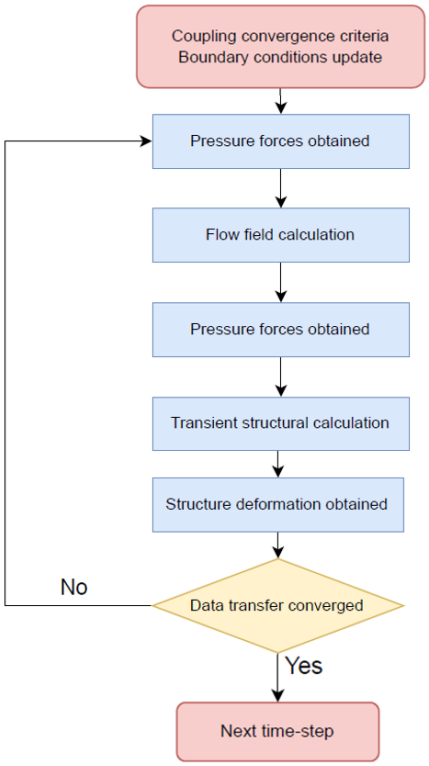

Figure 7. Coupling procedure within one time-step.

To realise the data exchange at the topology level, the ANSYS System-Coupling procedure maps points between the meshes of the models and then interpolates the values of the data exchanged between them. Owing to that, no compatibility of numerical models is required between models of different solvers. The diagram in Figure 7 illustrates the data exchange loop within one-time step, where flow calculations are realised first. In the performed simulations, the number of data exchange iterations was limited to 10, which was sufficient to ensure good convergence of results between solvers at the end of each time step. The step was 0.02 s, and the time of the whole simulation was set to 2.0 s. These values guaranteed convergence of the solutions within an acceptable computational time required by the simulations.

ANALYSIS RESULTS AND DISCUSSION

Based on the experimental testing results, a hypothesis was made assuming that the presence of the hysteresis loop was related to the conditions of contact between the valve discs. To verify the hypothesis, it was decided to perform a series of simulations at different friction factors for the contact conditions. The simulations were carried out on the model representing Valve 1 (Table 1), which was adopted as the reference model. For comparison purposes, a hysteresis width parameter calculated according to Eq. (5) was introduced.

$$H = \left(\frac{\max(p_{up} - p_{down})}{p_{max}}\right) \cdot 100\% \tag{5}$$

where:
p_{up} – pressure during the increase in the flow rate
p_{down} – pressure during the decrease in the flow rate
p_{max} – maximum pressure generated by the valve

The values obtained in this manner are presented on the bar chart in Figure 8.

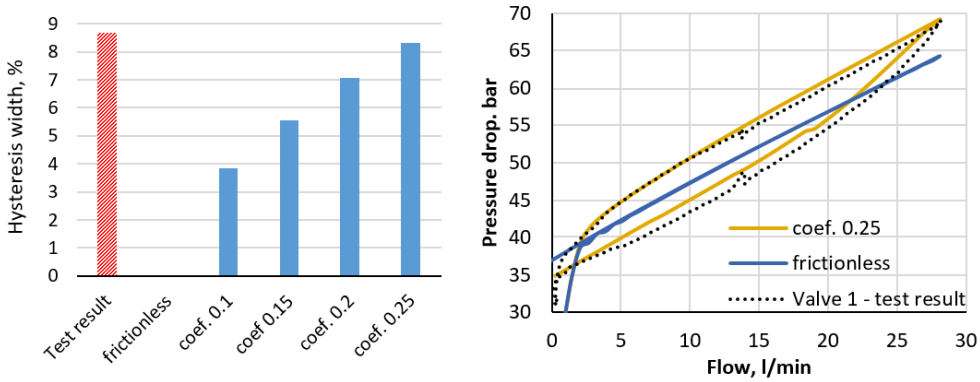

Figure 8. Comparison of Valve 1 simulation results for different friction factor values with experimental results.

The assumption of a frictionless contact in the simulation results in a complete lack of hysteresis of the characteristic curve and an underestimated level of the pressure generated by the valve. The very poor correlation of such a model with the experiment indicates that this assumption is far from reality. As the friction factor rises, the hysteresis field gets wider. The best correlation in terms of the hysteresis loop width and the valve stiffness (level of generated pressure) was achieved for the value of 0.25. The value may be considered as high, but it does occur for the steel-steel contact in an oil lubricant [28].

The flow rate decrease curve obtained in the simulation (coef. 0.25) consists of 2 segments with different slopes, which is marked in Figure 9. The point of the change in slope is distinctly visible, which is not the case for the experimental curve. The reason behind it is the change in the nature of friction (from static to kinetic) on a considerable area of the discs. The Coulomb friction model implemented in the software is characterised by a step transition between different friction types [29]. The results indicate that it is the appearance of static friction after the change in the direction of the motion of the valve discs that is the cause of the hysteresis loop generation by the numerical model. The effect can be seen in Figure 9.

The segment with a bigger slope corresponds to static friction immediately after the change in the direction of pressure changes, which is related to the change in the direction of the deformation of the discs. A drop in pressure first causes a build-up of tangential forces between the discs; the moment that fully-developed friction is achieved, there is a sharp jump to the level of kinetic friction forces. It can be seen that the phase of the motion of the discs related to the kinetic friction effect is characterised by an equal rate of changes in pressure on both the pressure increase and decrease side. This also explains the lack of hysteresis for the case without friction.

In order to facilitate the numerical solution convergence, the elastic slip tolerance is used. This means introducing a certain tangential stiffness of contact in the state of static friction. The stiffness value is calculated automatically in the ANSYS program. However, it is possible to influence the slip value by controlling the elastic slip coefficient. The impact of this parameter on contact conditions and consequently on the shape of the generated flow characteristics was

investigated. The elastic slip coefficient was changed in the range from 0.005 to 0.1 without changing the other contact parameters, i.e. the friction factor, the augmented Lagrange formulations and others.

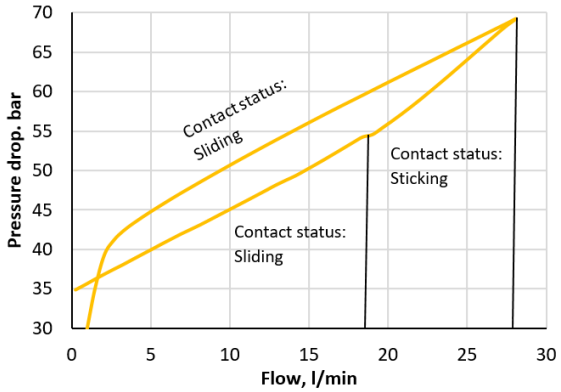

Figure 9. Basic status of contact between the valve discs in different regions of the characteristic curve.

For the coefficient limit values, the difference in the generated pressure levels did not exceed 1.0% and no significant effect was observed on the point of transition from the sticking to the sliding contact status.

As already mentioned, the point of the beginning of sliding in the contact between the discs cannot be determined on the experimental curve unambiguously. In order to better represent the shape of the characteristic curve of the flow rate decrease in the simulation results, attempts could be made with other friction models. To this end, the inclusion of the Stribeck effect in the friction model may be crucial. Next, attempts can also be made with more complex models, such as the LuGre model [29].

In order to confirm the correlation of the proposed modelling approach and the determined friction factor, it was decided to simulate Valve 2 (Table 1), which demonstrated the smallest hysteresis field among the configurations under analysis. The results obtained from the simulation (solid line) and from the testing (dashed line) for Valve 2 and Valve 1 are presented in Figure 10.

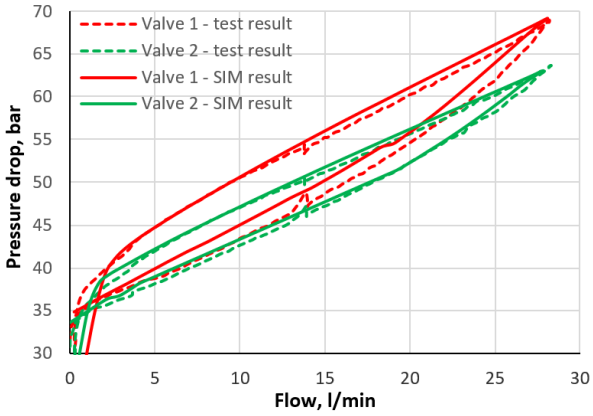

Figure 10. Results of the correlation of the flow characteristic curves obtained from simulations with the results obtained from the experiment for Valve 1 and Valve 2.

The characteristics obtained from the numerical models for Valve 1 and Valve 2 show satisfactory correlation, both in the context of mapping the pressure level generated by the valve and in terms of the hysteresis field width. Despite the significant difference in the disc stack composition, the valves demonstrated similar stiffness. At the maximum flow rate, the disc stack opening totalled 0.100 mm and 0.115 mm for Valve 1 and Valve 2, respectively. The pressure distribution and the velocity field for the valves are shown in Figure 11 and Figure 12.

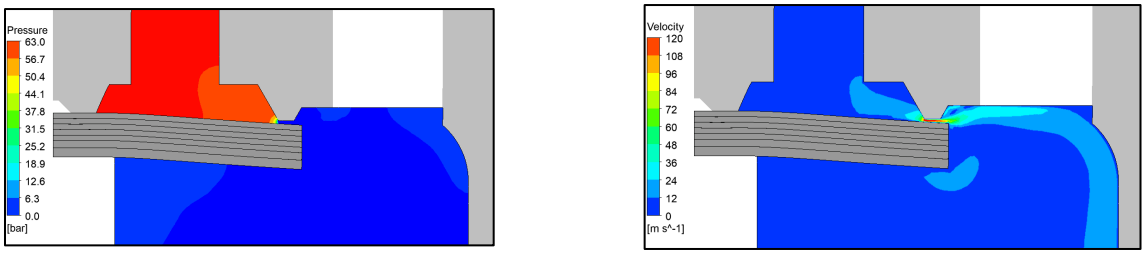

(a) (b)

Figure 11. Pressure (a) and velocity distribution in the symmetry plane for Valve 1 at the flow rate of 25 l/min.

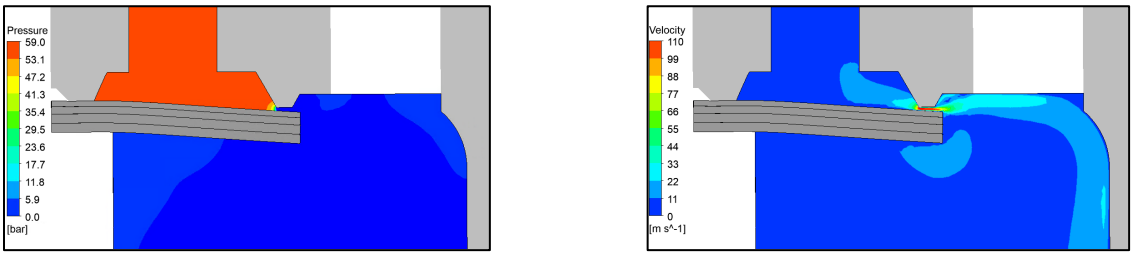

(a) (b)

Figure 12. Pressure (a) and velocity (b) distribution in the symmetry plane for Valve 2 at the flow rate of 25 l/min.

In the next step, a decision was made to investigate the impact of the discs preload on the width of the hysteresis field. Due to the fact that the clamping force in the process of the valve pin crimping is constant, the degree of the discs preload was changed by varying the Hub-Land height. The reference model (Valve 1) was characterised by the difference of 0.20 mm between the Hub-Land levels. This is a high value for the analysed valve type. A series of analyses were performed with the difference between the levels reduced every 0.05 mm. The results are gathered in Figure 13.

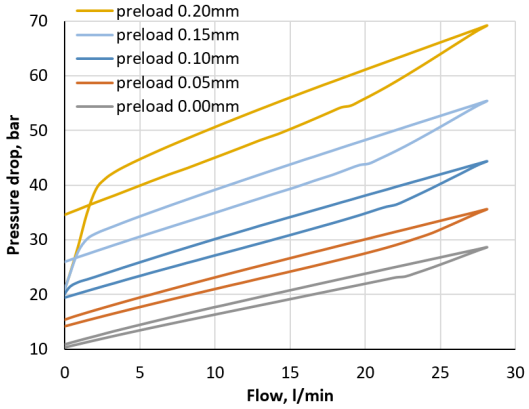

Figure 13. Pressure-flow rate chart for Valve 1 for different conditions of the disc stack preload.

The anticipated impact of a lower preload of the discs can be seen on the chart in the form of a shift of the curves towards lower pressures. However, the slope of the curves remains unchanged. The hysteresis fields between the flow rate increase and decrease get smaller with a drop in the pressures generated by the valve. The hysteresis loop width (Eq. 1) for the analysed conditions of the valve composition varies in the range from 8.3% (0.20 mm) to 5.7% (0.00 mm). This means that the degree of the disc stack preload is a factor affecting the hysteresis level. Unfortunately, any interference with this parameter has a significant impact on the overall level of generated pressure.

Figure 14 presents Valve 1 characteristic curves for the flow rate of 30 and 60 l/min. A rise in the flow rate amplitude had no significant effect on the relative width of the hysteresis field determined from Eq. (5). This confirms the conclusion that the hysteresis loop occurrence is due to the conditions of the valve composition, as these conditions translate into the state of contact between the discs.

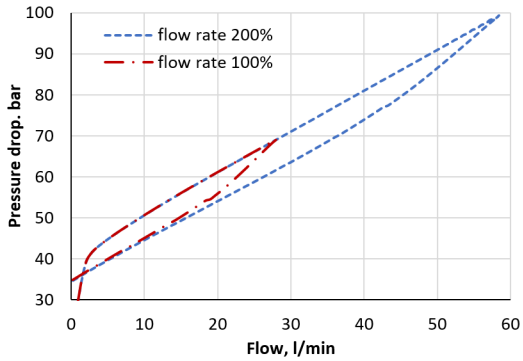

Figure 14. Pressure-flow rate chart for Valve 1 for the flow rate amplitude of 30 and 60 l/min.

CONCLUSION

This paper presents investigations on the occurrence of hysteresis of the damping curve of a shock absorber valve. The performed FSI simulation clearly confirms that hysteresis observed in the experimental pressure drop–flow rate curves originate from the frictional forces at the interface of the discs. Experimental validation of the FSI model performed based on two different designs of the valve (see Figure 10), revelated that even with the use of the relatively simple

mathematical model of friction (Coulomb friction + elastic slip behaviour within the FSI simulation) it is possible to accurately reproduce hysteretic behaviour of the valve.

Analysis of pressure drop–flow rate curves obtained experimentally as well as mathematically (see Figure 9), allowing for the identification of the following lubrication regimes: boundary lubrication and mixed lubrication. At the low flow rates and valve openings, friction is exerted due to surface asperities remaining in contact with each other. Within this regime, frictional forces behave elastically. At higher openings of the valve, contact at the level of asperities is gradually lost, resulting in the non-elastic behaviour of frictional forces. Described characteristics of the friction indicate that for system and control intended models of a shock absorber, the application of Dahl's friction model might be particularly useful as it focuses on reproducing the pre-sliding part of the contact motion. Due to testing capabilities, it was not possible to observe the dependency of the friction force on the velocity of the contact motion. However, it is hypothesised by the authors that due to relatively low displacements of adjacent surfaces, hydrodynamical effects happening at higher Hersey numbers would be difficult to develop and therefore affect the frictional forces.

High hysteresis can be expected under high preload or with high stiffened stack valve designs. For this type of valve, friction might significantly alter the initially intended characteristics of the valve. On the other hand, large valve deflections and openings which might take place at high flow rates are not affected by the frictional forces (Figure 14).

ACKNOWLEDGEMENT

The research was co-financed under the grants nos. 11/DW/2017/01/1 and RJO15/SDW/001-61/US supported by the Ministry of Science and Higher Education in Poland. Additionally, the authors are grateful to the Tenneco Inc. Company for their good cooperation and the opportunity to publish the research results.

REFERENCES

[1] J.A. Calvo, B. López-Boada, J.L.S. Román, and A. Gauchía, "Influence of a shock absorber model on vehicle dynamic simulation," *Proc. Inst. Mech. Eng. D: J. Automob. Eng.*, vol. 223, no. 2, pp. 189–203, 2009, doi: 10.1243/09544070jauto990.

[2] M.R. Ahmed, A.R. Yusoff, and F.R.M. Romlay, "Adjustable valve semi-active suspension system for passenger car," *Int. J. Automot. Mech. Eng.*, vol. 16, no. 2, pp. 6470–6481, 2019, doi: 10.15282/ijame.16.2.2019.2.0489.

[3] P. Czop, and J. Gniłka, "Reducing aeration and cavitation effect in shock absorbers using Fluid-structure interaction simulation," *Comput. Assist. Methods Eng. Sci.*, [S.l.], vol. 23, no. 4, pp. 171–189, Sept. 2017. ISSN 2299-3649.

[4] N. Pavlov, "Influence of shock absorber temperature on vehicle ride comfort and road holding," *MATEC Web of Conferences*, vol. 133, no. 02006, 2017, doi: 10.1051/matecconf/201713302006.

[5] D. Miroslav, D. Djordje, and M. Milan, "A contribution to research of the influence of degradation of vehicle vibration parameters on thermal load of shock absorbers," *Istrazivanja i Projektovanja Za Privredu*, vol. 11, no. 1, pp. 23–30, 2013, doi: 10.5937/jaes11-3270.

[6] H.H. Lang, and L. Segel, "The mechanics of automotive hydraulic dampers at high stroking frequencies," *Veh. Syst. Dyn.*, vol. 10, no. 2–3, pp. 82–85, 1981, doi: 10.1080/00423118108968640.

[7] A.L. Audenino, and G. Belingardi, "Modelling the dynamic behaviour of a motorcycle damper," *Proc. Inst. Mech. Eng. D: J. Automob. Eng.,* vol. 209, no. 4, pp. 249-262, 1995, doi: 10.1243/PIME_PROC_1995_209_212_02.

[8] K. Tian *et al.*, "A piecewise hysteresis model for a damper of HIS system," *Shock Vib.*, pp. 1–11, 2016, doi: 10.1155/2016/9091783.

[9] X.C. Akutain, J. Vinolas, J. Savall, and J. Biera, "A parametric damper model validated on a track," *Int. J. Heavy Veh. Syst.*, vol. 13, no. 3, pp. 145, 2006, doi: 10.1504/ijhvs.2006.010015.

[10] A. Simms, and D. Crolla, "The influence of damper properties on vehicle dynamic behaviour," *SAE Transactions*, vol. 111, pp. 505–516, 2002, doi: 10.4271/2002-01-0319.

[11] X. Wen-Xue, L. Zhen-Hua, and Z. Ping-Zhang, "FSI simulation and experimental validation of non-linear dynamic characteristics of a gas-pressurised hydraulic shock absorber," *IOP Conf. Ser.: Mater. Sci. Eng.*, vol. 576, no. 012014, 2019, doi: 10.1088/1757-899X/576/1/012014.

[12] S. Hong-Yu, G. Cheng, L. Shuang, and W. Ming-Ming, "Fluid-structure interaction of shock absorber for structure-borne noise based on compensation valve opening," In ISBDAI '18: Proceedings of the International Symposium on Big Data and Artificial Intelligence, 2018, pp. 129-134, doi: 10.1145/3305275.3305301.

[13] U. Ferdek, and J. Luczko, "Modeling and analysis of a twin-tube hydraulic shock absorber," *J. Theor. Appl. Mech., vol.* 50, no. 2, pp. 627-638, Warsaw, 2012.

[14] P. Czop *et al.*, "A computational fluid flow analysis of a disc valve system," *J. KONES*, pp. 117-122, 2011,.

[15] R. Sánchez *et al.*, "Assessment of the fluid-structure interaction capabilities for aeronautical applications of the open-source solver SU2," In Conference: VII European Congress on Computational Methods in Applied Sciences and Engineering, 2016, pp. 1498-1529, doi: 10.7712/100016.1903.6597.

[16] C. Kassiotis, A. Ibrahimbegovic, R. Niekamp, and HG. Matthies, "Non-linear fluid–structure interaction problem. Part I: implicit partitioned algorithm, non-linear stability proof and validation examples," *Comput. Mech.*, vol. 47, no. 3, pp. 305–323, 2010, doi: 10.1007/s00466-010-0545-6.

[17] C. Farhat, KG. van der Zee, and P. Geuzaine, "Provably second-order time-accurate loosely-coupled solution algorithms for transient non-linear computational aeroelasticity," *Comput. Methods Appl. Mech. Eng.*, vol. 195, no. 17–18, pp. 1973–2001, 2006, doi: 10.1016/j.cma.2004.11.031.

[18] L. Wiesent, M. Wagner, and M. Geith, "Simulation of Fluid-Structure Interaction between injection medium and balloon catheter using ICFD," presented at 11th European LS-Dyna Conference 2017, Salzburg, Austria, 2017.

[19] D. Bhuyan, and K. Kumar, "Design and analysis of base valve of twin tube dampers," *Appl. Mech. Mater.*, vol. 852, pp. 504-510, 2016, doi: 10.4028/www.scientific.net/AMM.852.504.

[20] S. Hong-Yu, G. Cheng, L. Shuang, and W. Ming-Ming, "Fluid-structure interaction of shock absorber for structure-borne noise based on compensation valve opening," *Proceedings of the International Symposium on Big Data and Artificial Intelligence*, 2018, pp. 129–134, doi: 10.1145/3305275.3305301.
[21] ANSYS Fluent theory guide release 2019 R3, ANSYS, Inc., Jun. 2020.
[22] D.C. Wilcox, "Formulation of the k-w turbulence model revisited," *AIAA Journal*, 2008, vol. 46, no. 11, pp. 2823–2838, doi: 10.2514/1.36541.
[23] M.A. Abd Halim, N.A.R. Nik Mohd, M.N. Mohd Nasir, and M.N. Dahalan, "Experimental and numerical analysis of a motorcycle air intake system aerodynamics and performance," *Int. J. Automot. Mech. Eng.*, 2020, vol. 17, no. 1, pp. 6470–6481, doi: 10.15282/ijame.17.1.2020.10.0565.
[24] S. Guillas, N. Glover, and L. Malki-Epshtein, "Bayesian calibration of the constants of the k–ε turbulence model for a CFD model of street canyon flow," *Comput. Methods Appl. Mech. Eng.*, vol. 279, pp. 536-553, 2014, doi: 10.1016/j.cma.2014.06.008.
[25] G. Yoon, "Topology optimisation method with finite elements based on the k- ε turbulence model," *Comput. Methods Appl. Mech. Eng.*, vol. 361, no. 112784, 2020, doi: 10.1016/j.cma.2019.112784.
[26] P. Le Tallec, and J. Mouro, "Fluid structure interaction with large structural displacements," *Comput. Methods Appl. Mech. Eng.*, vol. 190, no. 24–25, pp. 3039-3067, 2001, doi: 10.1016/S0045-7825(00)00381-9.
[27] S.K. Chimakurthi, S. Reuss, M. Tooley, and S. Scampoli, "ANSYS workbench system coupling: a state-of-the-art computational framework for analysing multiphysics problems," *Eng. Comput.*, vol. 34, no. 2, pp. 385–411, 2017, doi: 10.1007/s00366-017-0548-4.
[28] R.T. Barrett, *Fastener design manual*. Lewis research center. Cleveland, Ohio, NASA Reference Publication 1228; 1990.
[29] V. Geffen, "A study of friction models and friction compensation", Traineeship report, Eindhoven, December, 2009.